and $[Eb]_d$ by

$$Eb_i = Eb[kd(i)] - e_i, \qquad \text{with } i \preccurlyeq n_\Delta. \tag{30}$$

$Eb[kc(i)]$ and $Eb[kd(i)]$ are components of matrix $[Eb]_p$.

III. Results

A simulation program has been developed using the operators of dilatation and shrinkage defined in Section II. Different configurations and particularly the structure given in Fig. 4 were tested. The lines are microstrip 0.2 mm wide, and the spacing between the lines in the coupling region is $s = 0.1$ mm. The dielectric substrate has a height $h = 1.55$ mm, a strip thickness $t = 35$ μm, and a dielectric constant $\epsilon_r = 3.0$.

The circuit is divided into tubes of one, two, and three lines with the equivalent impedance matrices given below [5].

For a tube of one line:

$$[R]_1 = [162]\ \Omega$$

for a tube of two lines:

$$[R]_2 = \begin{bmatrix} 159 & 97 \\ 97 & 159 \end{bmatrix} \Omega$$

for a tube of three lines:

$$[R]_3 = \begin{bmatrix} 158 & 95 & 69 \\ 95 & 155 & 95 \\ 69 & 95 & 158 \end{bmatrix} \Omega.$$

The circuit is fed through point (a) by a generator delivering the signal represented in Fig. 5. While simulating the circuit, the input signal is approximated by the curve given in Fig. 6. Point (d) is open ($Zd = \infty$) and the other points are terminated by 50-Ω loads ($Zb = Zc = Ze = Zf = 50\ \Omega$). The output signals are filtered by the oscilloscope used in the measurements. Therefore, we have smoothed the theoretical results by a theoretical filter with $RC = 50$ ps.

The simulation results (dashed curves) and those of the measurements (continuous curves) are given in Fig. 7. The excellent agreement between the experimental and theoretical results proves the validity of the method.

IV. Conclusions

In a given integrated or printed circuit, some lines may be coupled along some part of their length, and are termed partially coupled lines. The method proposed in this paper provides a straightforward time-domain analysis of this kind of line. It is based on the concepts derived from analysis of continuous lines, and readily applies to any number of nonuniformly coupled lines. Dividing a structure of partially coupled lines into tubes allows one to use transient analysis methods described for continuous coupled lines (modal analysis, characteristics method).

In order to solve the problem of interfaces between tubes of different order, we have introduced two operators, called dilatation and shrinkage. By testing different partially coupled lines, close agreement with theoretical results is obtained, proving the validity of the proposed method. The number of lines is not a limiting factor, and the method can be applied to nonuniformly coupled lines [7]. In this case, the nonuniformly coupled lines can be divided into cascaded tubes with different propagation parameters.

Some authors use methods based on a multiport conception and the scattering matrix to solve the junction problem [8]. The dilatation and shrinkage operators can also be used in these cases when the lines are discontinuous.

References

[1] J. Chilo and T. Arnaud, "Coupling effect in the time domain for interconnecting bus in high speed GaAs logic circuits," *IEEE Trans. Electron Devices*, vol. ED-31, pp. 347–352, Mar. 1984.

[2] F. Y. Chang, "Transient analysis of lossless coupled transmission lines in nonhomogeneous dielectric medium," *IEEE Trans. Microwave Theory Tech.*, vol. MTT-18, pp. 616–625, Sept. 1970.

[3] P. I. Kuznetsov and R. L Stratonovich, *The Propagation of Electromagnetic Waves in Multiconductor Transmission Lines*. New York: Macmillan, 1964.

[4] T. Razban, C. Monllor and P. Vincensini, "A new method for transient analysis of discontinuous coupled lines," in *Proc. 16th European Microwave Conf.*, 1986, pp. 517–522.

[5] J. Chilo, "Les interconnexions dans les circuits integrés logiques rapides: outils de modélisation et d'analyse temporelle," Thèse de doctorat d'état, INP Grenoble, Nov. 1983.

[6] F. R. Branin, "Transient analysis of lossless transmission lines," *Proc. IEEE*, vol. 55, pp. 2012–2013, Nov. 1976.

[7] Y. E. Yang, J. A. Kong, and Q. Gu, "Time-domain perturbational analysis of nonuniformly coupled transmission lines," *IEEE Trans. Microwave Theory Tech.*, vol. MTT-33, pp. 1120–1129, Nov. 1985.

[8] A. K. Agrawal, H. M. Fowles, L. D. Scott, and H. Gurbaxani, "Application of modal analysis to the transient response of multiconductor transmission lines with branches," *IEEE Trans. Electromagn. Compat.*, vol. EMC-21, pp. 256–262, Aug. 1979.

FM Noise in Multiple-Device Oscillators

S. SARKAR AND O.S. GUPTA

Abstract —**The FM noise in a multiple-device oscillator is analyzed. It is shown that FM noise depends on the circuit parameters and the number N of the constituent devices. For a circuit-dependent critical value of N, FM noise is maximum and it is proportional to $N^{-\frac{1}{2}}$ when N is very large.**

I. Introduction

Kurokawa's analysis [1] shows the FM noise in a multiple-device oscillator to be inversely proportional to the external Q and the number of active devices which constitute the oscillator. The analysis, however, assumes external Q to be independent of the number of active devices. More recently, it has been observed that the external Q of a multiple-device oscillator decreases as the active devices are increased in number [2]–[4]. In view of these observations, this paper analyzes the circuit dependence of FM noise in a multiple-device oscillator.

II. RMS Frequency Deviation

Typically, a multiple-device oscillator [1] consists of a number N of identical negative-conductance devices, each provided with a stabilizing conductance G_0 and equally coupled to a power-combining cavity. The cavity is equivalent to a parallel combination of a loss conductance G_c that includes circuit losses other than those in the G_0's, a capacitance C_c, an inductance, and an equivalent load conductance $n_o^2 G_L$, where G_L is the load conduc-

Manuscript received August 18, 1986; revised November 25, 1986.

The authors are with the Department of Electronics and Communication Engineering, University of Roorkee, Roorkee 247 667 India.

IEEE Log Number 8613465.

tance at the output port of the oscillator and n_o is the output coupling coefficient. If $-g_{opt}$ is the optimum negative conductance of an individual device and n_t is the device–cavity coupling coefficient, then high power-combining efficiency can be achieved, when $G_0 \gg g_{opt}$ and $G_c \ll n_t^2 N g_{opt}$ [1]. Usually, a multiple-device oscillator circuit is optimized for maximum power output. This can be achieved by adjusting the coupling coefficients n_t and n_o. In actual practice, however, n_t is not an adjustable parameter, since it is determined by the dimensions and position of an individual device mount. On the other hand, n_o can be made adjustable by coupling the oscillator output to the load through adjustable coupling components such as turners. When the high power-combining efficiency requirements mentioned above are satisfied and the output coupling coefficient is adjusted for maximum power output:

$$n_o \approx n_t \sqrt{\frac{N g_{opt}}{GL}} \tag{1}$$

then the resulting external Q at an operating frequency of f_o is [5]

$$Q_{ext} \approx \frac{2\pi f_o}{g_{opt}} \left(C_D + C_c / n_t^2 N \right) \tag{2}$$

where C_D is the capacitance of an individual device. Thus, (1) and (2) indicate that, as the devices are increased in number Q_{ext} decreases, while n_o increases.

For a single-device power output of P_d, it can be shown that the power-combining efficiency η and the power output P_o of the multiple-device oscillator are

$$\eta = \left(1 + \frac{G_c}{n_t^2 N g_{opt}} \right)^{-1} \tag{3}$$

and

$$P_o = NP_d \bigg/ \left(1 + \frac{G_c}{n_t^2 N g_{opt}} \right). \tag{4}$$

FM noise in an oscillator is conveniently expressed by the rms frequency deviation in a given band width. For the oscillator under consideration, the rms frequency deviation in a bandwidth B is [1]

$$\Delta f_{rms} = \frac{f_o}{Q_{ext}} \sqrt{\frac{KTB}{P_o \eta}} \tag{5}$$

where K is Boltzman's constant and T is the equivalent noise temperature of an individual device. Substituting (2)–(4) into (5),

$$\Delta f_{rms} = \frac{G_c + n_t^2 N g_{opt}}{2\pi \left(C_c + n_t^2 N C_D \right)} \sqrt{\frac{KTB}{NP_d}}. \tag{6}$$

If $\overline{v_n^2}$ is the mean square noise voltage in a bandwidth B, then

$$KTB = \frac{\overline{v_n^2}\, g_{opt}}{4}. \tag{7}$$

Substituting (7) into (6),

$$\Delta f_{rms} = \frac{G_c + n_t^2 N g_{opt}}{2\pi \left(C_c + n_t^2 N C_D \right)} \sqrt{\frac{\overline{v_n^2}\, g_{opt}}{4NP_d}}. \tag{8}$$

An examination of (8) shows that, in general, as the devices are increased in number, the rms frequency deviation first increases, then it reaches a peak, and then decreases as the active devices are increased in number.

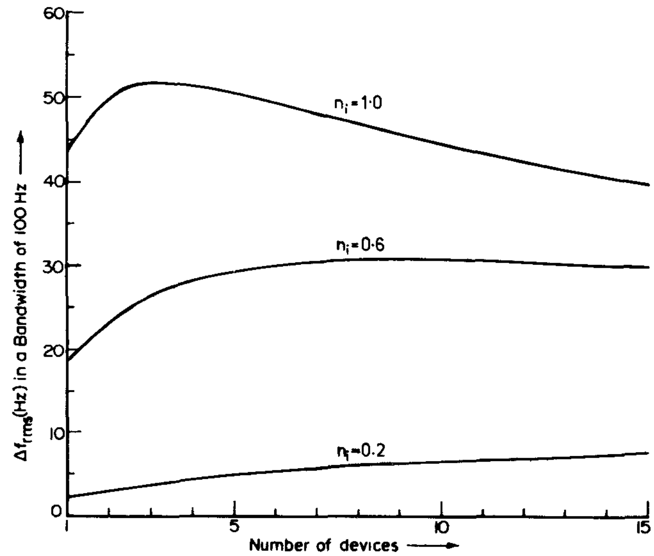

Fig. 1. Dependence of rms frequency deviation on the number of active devices

Commonly, either Gunn or IMPATT diodes are used in multiple-device oscillators. Measurements show that, depending on the circuit and device used, in a bandwidth of 1 kHz, the rms frequency deviations in the single-device Gunn and IMPATT oscillators vary from a few Hz to several hundred Hz [6]. If the rms frequency deviation is 43.31 Hz in a bandwidth of 100 Hz, when only one Gunn diode of $g_{opt} = 3$mmho, $C_D = 0.3$ pF, and $P_d = 50$ mW operates in a circuit where $G_c = 0.01$ mmho, $C_c = 1.0$ pF, and $n_t = 1.0$ the $\overline{v_n^2}$ of the diode as calculated from (8) is 9×10^{-13} V^2. Fig. 1 illustrates the dependence of the rms frequency deviation on the number of such active devices in the assumed oscillator circuit for three different values of n_t. It can be seen that the number N_{peak} of active devices for which the peak in rms frequency deviation occurs is dependent on the coupling coefficient. N_{peak} is larger for small coupling coefficient. As a consequence of this, for too small a coupling coefficient (e.g., $n_t = 0.2$), N_{peak} may be beyond the device-accommodating limit of the multiple-device oscillator. In that case, the rms frequency deviation simply increases as the active devices are increased in number.

Assuming $G_c \ll n_t^2 N g_{opt}$, from (8) it may be shown that

$$N_{peak} \approx \frac{1}{n_t^2} \frac{C_c}{C_D}. \tag{9}$$

The dependence of N_{peak} on the coupling coefficient is shown in Fig. 2 for three different values of C_c/C_D.

Normally, the active devices of a multiple-device oscillator are increased in number with the objective of improving the power output. If N_{peak} of a multiple-device oscillator is small and well within the device-accommodating capacity of the oscillator structure, then in addition to the achievement of the above objective, improvement in FM noise is also achieved as the active devices are increased in number beyond N_{peak}. It has been already mentioned that N_{peak} can be reduced by increasing the coupling coefficient (Fig. 2). Such a reduction of N_{peak} of course increases the rms frequency deviation, but at the same time makes it more sensitive to a change in the number of active devices (Fig. 1). Also, as indicated by (3), a larger coupling coefficient yields a higher power-combining efficiency. Thus, in a multiple-device

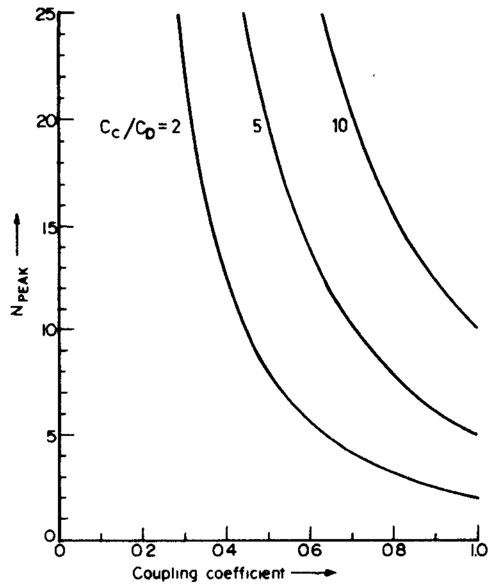

Fig. 2. N_{peak} as a function of coupling coefficient n_i. The parameter is the C_c/C_D ratio.

oscillator of high power-combining efficiency, after a few devices are added, the rms frequency deviation may be expected to decrease rapidly as the active devices are further increased in number. However, much depends on the C_c/C_D ratio. If this ratio is small, the rms frequency deviation may fall without undergoing any rise when the active devices are increased in number. For example, when the C_c/C_D ratio is 2 and the coupling coefficient is 1.0, N_{peak} is 2 (Fig. 2). In such a case, as the active devices of the multiple-device oscillator are increased in number from the minimum of 2, the rms frequency deviation only decreases and does not rise at all. On the other hand, if the coupling coefficient is small and the C_c/C_D ratio is large enough for N_{peak} to be larger than the maximum number of devices that can be accommodated by the oscillator structure, the rms frequency deviation continues to increase as the active devices are increased in number. The curve for $n_i = 0.2$ in Fig. 1 is such an example of a multiple-device oscillator structure with fewer than 15 devices.

If the active devices are increased in number to the extent that

$$n_i^2 N g_{opt} \gg G_c \tag{10}$$

and

$$n_i^2 N C_D \gg C_c \tag{11}$$

then from (8)

$$\Delta f_{rms} \simeq \frac{g_{opt}}{2\pi C_D}\sqrt{\frac{\overline{v_n^2}\, g_{opt}}{4NP_d}} \tag{12}$$

Thus as shown by (12), when a multiple-device oscillator is comprises a very large number of active devices, its rms frequency deviation is independent of the coupling coefficient and is inversely proportional to the square root of the number of constituent active devices.

III. Conclusions

Considering the dependence of external Q on circuit and active device parameters, an analysis of FM noise in a multiple-device oscillator is presented. The analysis shows that, with proper selection of circuit parameters, the rms frequency deviation in such an oscillator decreases rapidly with an increase in the number of active devices. Increased coupling between the active devices and the power-combining cavity increases the rms frequency deviation. This influence of device–cavity coupling, however, diminishes as the active devices are increased in number.

References

[1] K. Kurokawa, "The single-cavity multiple-device oscillators," *IEEE Trans. Microwave Theory Tech.*, vol. MTT-19, pp. 793–801, Oct 1971.

[2] R. Aston, "Techniques for increasing the bandwidth of a TM_{010}-mode power combiner," *IEEE Trans. Microwave Theory Tech.*, vol. MTT-27, pp. 479–482, May 1979.

[3] Y.E Ma and C Sun, "1-W millimeter-wave Gunn diode combiner," *IEEE Trans. Microwave Theory Tech.*, vol. MTT-28, pp. 1460–1463, Dec 1980.

[4] S. Nogi and K. Fukui, "Locking behavior of a microwave multiple-device ladder oscillator," *IEEE Trans. Microwave Theory Tech.*, vol. MTT-33, pp. 253–262, Mar 1985.

[5] S. Sarkar and O.S Gupta, "Dependence of multiple-device oscillator injection locking range on the number of constituent devices," *IEEE Trans. Microwave Theory Tech.*, vol. MTT-34, pp 839–840, July 1986.

[6] J. Josenhans, "Noise spectra of Read diode and Gunn oscillators," *Proc. IEEE*, vol. 54, pp. 1478–1479, Oct. 1966.

Measurements of Microstrip Effective Relative Permittivities

STEVE DEIBELE, STUDENT MEMBER, IEEE, AND JAMES B. BEYER, SENIOR MEMBER, IEEE

Abstract —**This paper presents normalized wide-bandwidth measurements of microstrip effective relative permittivities (ϵ_{eff}) which were made on large-scale microstrip models. The experimental techniques are discussed, and the data are compared to the predictions of two recent closed-form design equations. These results agree favorably with the predictions of Kirschning and Jansen's model. In addition, suggestions concerning frequency limitations of microstrip use and comments on the reliability of CAD packages for microstrip circuits are made.**

I. Introduction

Increased interest has recently been expressed in the characterization of microstrip, one of the popular planar transmission lines. Microstrip does not support transverse electromagnetic (TEM) waves and is hence dispersive. Several researchers [1]–[6] have employed both approximate and rigorous numerical techniques to calculate the phase velocities and the "impedances," but the rigorous techniques are quite involved and require too much computer time to be used directly in computer-aided design (CAD) applications [7]. Furthermore, the approximate techniques have limited regions of validity. Recently, two groups of researchers, Kirschning and Jansen [7] and Hammerstad and Jensen [8], addressed this problem by providing closed-form

Manuscript received September 29, 1986; revised January 17, 1987. This work was supported in part by the Hewlett-Packard Company, Stanford Park Division.

The authors are with the Department of Electrical and Computer Engineering, University of Wisconsin, Madison, WI 53706.

IEEE Log Number 8613831.